Journal of Sustainable Metallurgy (2021) 7:1589–1602
https://doi.org/10.1007/s40831-021-00453-0

THEMATIC SECTION: 3RD INTERNATIONAL BAUXITE RESIDUE VALORISATION AND BEST PRACTICES CONFERENCE

Selective Recovery of Graphite from Spent Potlining (SPL) by Froth Flotation

Panagiotis M. Angelopoulos[1] · Nikolaos Koukoulis[1] · Georgios N. Anastassakis[1] · Maria Taxiarchou[1] · Ioannis Paspaliaris[1]

Received: 26 May 2021 / Accepted: 14 October 2021 / Published online: 29 October 2021

Abstract

Spent potlining (SPL) consists of the carbon cathodes (1st cut), aluminosilicate refractories, and the insulation lining of Hall–Héroult cells (2nd cut) used in aluminum smelting. SPL is classified as hazardous material due to its high content in soluble fluoride salts and the presence of cyanides. The 1st cut contains considerable amount of carbon in graphitic form that can exceed 65 wt%; however, during cell's dismantling process inevitable mixing with the 2nd cut occurs causing its contamination with undesirable aluminosilicates. The study investigates the selective recovery of graphite from SPL sample and its separation from mullite and quartz through flotation. Prior to this, SPL has been subjected to special chemical treatment to render it safe for use by minimizing cyanides and free fluorides content through leaching with H_2O_2 and NaOH, respectively. Flotation tests were carried out aiming at the maximization of carbon grade and recovery in the concentrate, while minimizing silicon content. The effect of pH, collector, and sodium silicate (depressant) dosage was investigated on two feeds of different granulometry (− 90 μm, 90–420 μm) and optimum conditions were determined. For pH 8 and kerosene dose of 500 g/t, carbon grade and recovery in the concentrate reached 85.6 wt% and 85.1% for the fine sample (− 90 μm), and 84 wt% and 94.9% for the sample with particle size 90–420 μm, respectively. The results clearly show that mullite and quartz were effectively separated since the silicon content was less than 1 wt% in both concentrates. Further grade improvement is possible through further size reduction of the concentrate and subsequent alkaline leaching towards elimination of fluoride salts and cryolite.

The contributing editor for this article was Yiannis Pontikes.

✉ Panagiotis M. Angelopoulos
pangelopoulos@metal.ntua.gr

[1] School of Mining Engineering and Metallurgy, National Technical University of Athens (NTUA), 9 Heroon Polytechniou Str, 15780 Zographou, Greece

Graphical Abstract

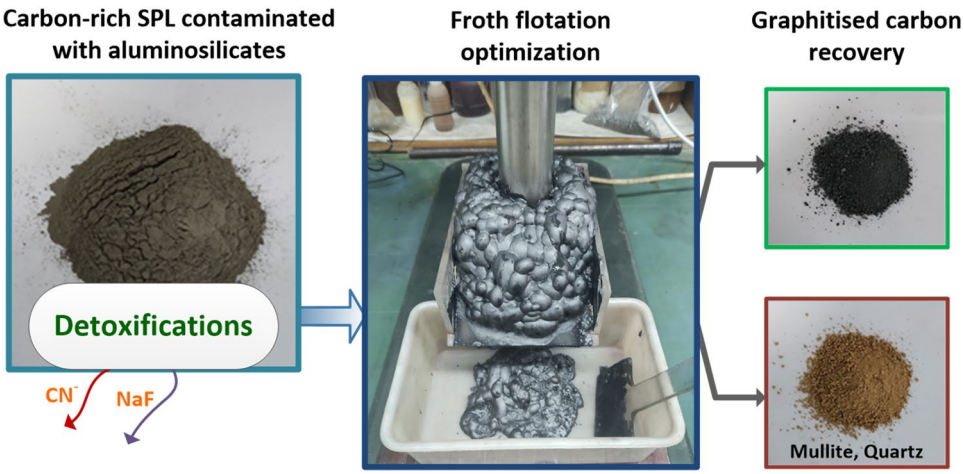

Keywords Spent potlining (SPL) · Graphitized carbon recovery · Froth flotation · SPL detoxification

Introduction

Spent potlining (SPL) constitutes a waste produced during dismantling of Hall–Héroult cells used in aluminum smelting; it consists of the carbon cathodes, as well as the aluminosilicate refractories and insulation lining of the cell, located above and below the collector bars, respectively. Dismantling process takes place every 3 to 8 years, depending on the operation conditions of the cell and the construction technique and materials, as carbonaceous cathode material degrades thus affecting the cell performance [1, 2]. The structure of SPL is mainly affected by carbon graphitization, sodium intercalation and other side reactions due to bath material penetration [3]. It is estimated that SPL generation rate is 22 kg per ton of aluminum produced; thus, according to the annual primary aluminum production, approx. 1.4 million tons of SPL were produced in 2019 [4].

In industry, the name for carbon-rich SPL waste is 1st cut because this part is the first to be stamped off the bottom of the cell, while the aluminosilicate-rich grade of the waste, which mainly consists of refractory bricks, is called 2nd cut. It is estimated that SPL sample consists of carbon cathode and refractory material by 55 and 45 wt%, respectively [5]. The dismantling process takes place through mechanical means; consequently, undesirable mixing of 1st and 2nd cut to a certain level is inevitable. SPL is considered toxic, mainly due to its contamination with fluoride salts and cyanides, which are water soluble; thus, they may be leached from landfilled material and contaminate ground water or water run-offs. SPL composition varies, but in most cases its fluoride content is up to 20 wt% and cyanide up to 1 wt% [2].

Table 1 Uses of SPL 1st and 2nd cut in other industries without prior treatment

Grade	Use	References
1st cut	As alternative fuel in Clinker production	[5, 9, 10]
	As alternative fuel in Thermal power plant	[5, 9]
	As reductant for the extraction of metals (Zn, Cd, Ld, Fe)	[11]
	As flux and alternative fuel in steel making	[12]
	As alternative fuel in iron making process	[13]
	As coke substitute in mineral wool production	[4]
	As reducing agent in ferrosilicon manganese alloy	[14]
	As coal substitute in dolomite calcination process	[15]
	As flux and reductant in carbothermic reduction of chromite	[16]
2nd cut	In red brick production	[5, 9]
	Si source for Al–Si alloy production in alumina reduction cell	[17]
	The addition to quarry materials in the raw feed of a cement kiln	[18]

Another issue with SPL is that it reacts exothermally with water, and the evolution of H_2 and CH_4 renders it potentially explosive [6]. This caused explosion in the SPL transferring ship "Pollux," on 19th of March, 1990 in Port Alfred, Quebec, Canada, resulting in the loss of two people.

The massive production of SPL, along with the contamination with hazardous components and the fact that landfilling is not considered a sustainable waste management solution anymore, has initiated the development of various processes that primarily aim in the detoxification of SPL and its recycling. Certain applications have been developed, where untreated 1st cut SPL is utilized as fuel, reductant or flux, and 2nd cut as Si source (Table 1). Such applications involve thermal treatment of the material, usually to temperature above 1000 °C, for cyanides to be oxidized and decomposed, and for fluoride salts to be either dissolved in melts and absorbed/adsorbed during the utilization process or produce useful CaF_2 [1]. However, the toxic and potentially explosive properties of SPL prerequisites special treatment before and during the transportation of the material to the treatment plant, thus increasing the treatment cost. For that purpose, other methods have been developed on the production site aiming at the SPL detoxification and the recovery of useful fluoride products. The LCL&L (Low Caustic Leaching & Liming) method involves water and low caustic leaching of SPL, and mild heat treatment at 180 °C for fluorides and cyanides extraction and destruction [7]. Another process, developed by Alcoa, involves calcination of SPL together with limestone and an anti-agglomeration additive towards cyanides destruction and transformation of NaF–AlF_3 to less soluble CaF_2 [6]. In China, Chalco-SPL-Process involves SPL mixing with limestone and coal cinder, and subsequent calcination in rotary kiln, while the SPL-bauxite sintering process suggests the incorporation of 1st cut in bauxite sintering [8].

A zero waste process has been developed and optimized in the frame of the SPL-CYCLE project for both 1st and 2nd cut samples (http://splcycle.zag.si/). The process consists of five separation and purification stages, which are (i) destruction of cyanides using H_2O_2 solution, (ii) extraction of fluoride salts using NaOH solution, (iii) filtration for solid/liquid separation, (iv) fluoride salts crystallization, and (v) flotation for purification purposes, resulting in the production of the following four marketable products: fluoride salts for aluminum production, graphitized carbon, aluminosilicates for refractory industry, and manufactured aggregate for construction [19]. The important advantages of the SPL-CYCLE process are as follows: (a) it is a really zero waste technology of no wastes or byproducts, and (b) it involves the recovery of carbon, which is highly valued material and can be used as source material in various applications; in case of high-purity carbon product, it can be recycled internally in aluminum metallurgy for the production of anodes.

In step (v) of the process, flotation aims at the separation of hydrophobic graphitized carbon from aluminosilicates that originate from its inevitable mixing with the 2nd cut during cell dismantling, after detoxification and fluoride salts removal.

The separation of graphite from various gangue minerals (e.g., feldspar, kaolin, quartz, mica, carbonates) has been investigated through flotation [20–24]. Actually, graphite is one of the minerals easiest to float with non-ionic collectors due to its natural hydrophobic properties. Among various non-ionic hydrocarbons, such as fuel oil, paraffin, and diesel oil, kerosene is generally considered as the best collector for graphite flotation, with methyl isobutyl carbinol (MIBC) being the most common and efficient frother [25]. The mechanism of graphite flotation has been established since long time ago and more information can be found elsewhere [26–28]. Flotation process had been used in the past for the selective recovery of graphite from 1st cut SPL sample containing aluminosilicates. This is normally due to the natural hydrophobicity of graphite, and the hydrophilic behavior of aluminosilicates. Schönfelder et al. used EKOF 452 collector in dose of 500 g/t and achieved the production of concentrate with carbon grade of 87 wt%, from a sample with initial content of 50.65 wt%, but they did not provide data regarding the carbon recovery [29]. The same collector along with Sodium Lauryl Sulfate (SLS) as frother was used by Tropenauer et al. for the separation of the carbon-rich part of SPL from aluminosilicate bricks; they achieved the increase of carbon grade from 44.30 in the feed to 72.06 wt% in the concentrate, but no information regarding recovery was provided too [30]. On industrial scale, it is reported that flotation is applied for SPL purification purposes at Yichun Smelter (China), but no other information regarding processing conditions and products properties are available [4, 8]. Despite the fact that flotation of graphite ores constitutes a well-known procedure, when it comes to SPL the nature of the parental material differs significantly compared to graphite ores that have been investigated so far; high alkalinity, impregnation with fluoride salts, presence of cyanides, and mixing with the aluminosilicate liner compose a complex flotation environment, which has not been investigated thoroughly yet, in terms of the process performance and the effect of major flotation parameters.

In addition to flotation, Li et al. investigated the washability of microcrystal mineral graphite using float–sink analysis in terms of granulometry for specific gravity ranging from 1.3 to 2.0 ± 0.1 [31]. The main gangue mineral was quartz in approx. 10% by weight; the recovery of graphite was almost 90 wt% with fixed carbon content 72.29 wt%. In the current paper, sink–float analysis was applied to four detoxified SPL samples of different granulometry (− 210 μm, 210–420 μm, 420–840 μm, and 840–1190 μm) for sample characterization.

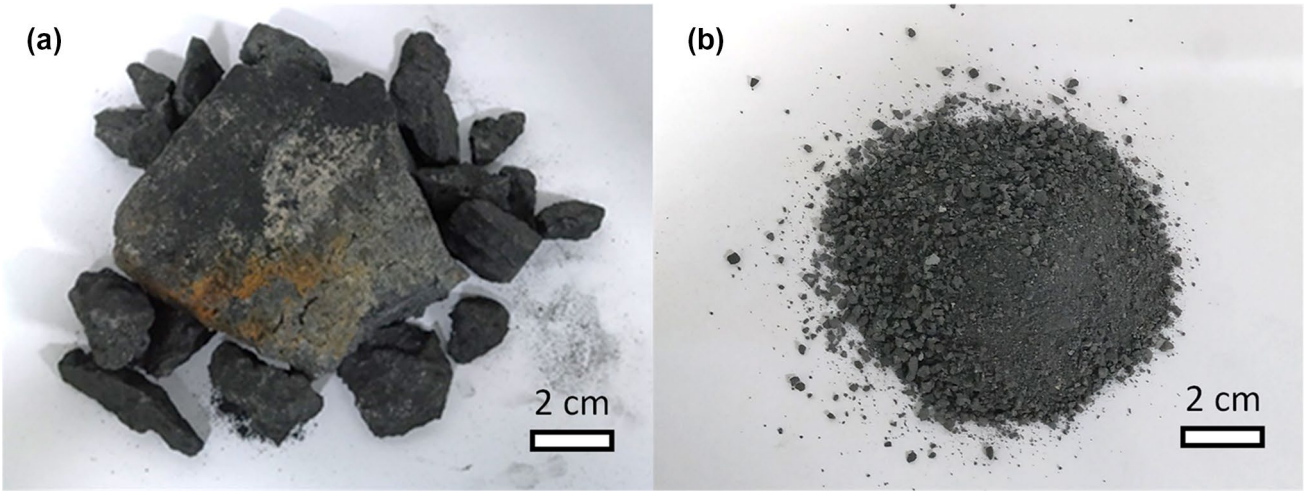

Fig. 1 SPL sample as received (**a**) and after size reduction (**b**)

The current study deals with the investigation of flotation as potential method to selectively recover graphite from 1st cut of SPL sample, targeting in parallel to minimize its content in aluminosilicates, which is primarily present in the form of mullite. Aiming to render SPL sample safe for use, it was first detoxified through leaching with H_2O_2 and NaOH to decompose and remove cyanides and free fluoride salts, respectively. Froth flotation tests were performed on samples with particle size − 90 µm and − 420 + 90 µm. Crucial process parameters were investigated, such as pH, as well as collector and depressant dose for siliceous minerals. The evaluation of the results was carried out through monitoring the carbon and silicon grade of the products and the recovery. Analytical, spectroscopy, and optical methods were employed to investigate the distribution of other impurities in the various products.

Materials and Methods

Materials Characterization

SPL sample has been obtained from a European aluminum refinery in block form. The chemical composition of the sample was analyzed using energy-dispersive X-ray fluorescence (ED-XRF) instrument Xepos (SPECTRO A. I. GmbH, Germany), while total carbon content (C_{tot}, wt%) was determined in LECO analyser (LECO 744 Series Analyzer, USA). Loss on Ignition (LOI) constitutes the weight loss that occurs when the sample is subjected to heating at 1000 °C for 1 h, and it is applied for quick estimation of sample content in volatiles, including organic matter and decomposition products [32, 33]. All chemical analyses were performed to pre-dried and fine ground samples. The free and total cyanides content was measured through a standard procedure, and their extraction was carried out by shaking a 20 g sample in 0.5 L of 1 M NaOH solution for 16 h [34]. Size distribution was analyzed in a Malvern Laser Particle Analyzer (Malvern Panalytical, UK) for samples with particle size below 400 µm, while sieving was applied to the coarser ones. Phase identification was carried out using X-ray powder diffraction device (Bruker D8 Advance device, Bruker Corp. USA) under the following conditions: scanning rate of 1° min^{-1}, 2θ range from 10° to 75°, and graphite-monochromatic CuKa radiation ($k = 0.15406$ Å). Rietveld process was applied for the quantitative determination of mineralogical phases in Profex software [35]. Samples' microstructure was investigated through Scanning Electron Microscopy (SEM) using SEM JEOL 6380 V at 20 kV, and local chemical microanalysis was carried out through energy-dispersive spectroscopy (EDS) feature. Grains' morphology was investigated in a Wild M5 stereomicroscope (Wild Heerbrugg, Switzerland).

The theoretical specific gravity of graphite, quartz, and mullite are 2.2, 2.65, and 3.2, respectively [36]. Tests were designed aiming to float graphite and sink other phases that possess higher specific gravity. A heavy liquid having specific gravity of 2.3 was prepared by mixing carbon tetrachloride (CCl_4, specific gravity 1.59) and 1, 1, 2, 2-tetrabromoethane ($C_2H_2BR_4$, specific gravity 2.96) in 63.45/36.55 volume ratio. The test was implemented in a 0.5 L beaker, where a representative SPL sample of 30 g was introduced into the beaker containing 350 ml of heavy liquid. The float and sink were collected, successively rinsed with alcohol and water, dried, and subsequently subjected to weight measurement and chemical analysis to determine carbon and silicon content in the floats, as well as the achieved recovery. The process was applied to four samples of the following particle

size range each: − 210 µm, 210–420 µm, 420–840 µm, and 840–1190 µm, having d50 of 96 µm, 298 µm, 581 µm, 964 µm and d80 of 194 µm, 375 µm, 763 µm, and 1112 µm, respectively.

Pre-treatment

The SPL sample was primarily crushed in jaw crusher (BB200, Retsch, Germany) and, subsequently, ground in pulveriser mill (LM2 model, Labtechnics Australia) to produce sample with granulometry below 2.36 mm (Fig. 1). Chemical analysis showed that both cyanide and fluoride content were high; aiming to reduce the content of the material in both toxic compounds, a two-step detoxification process that constitutes part of the SPL-Cycle flow-sheet was applied (Fig. 2). As described in Fig. 2, the detoxification process consists of two stages of material mixing with different solutions, followed by filtration and drying. First, SPL was mixed with 3 M H_2O_2 solution with cyanides been destroyed according to Eq. (1) [37]. Subsequently, 0.2 M NaOH solution was used for the decomposition and removal of fluoride salts in the form of sodium fluoride and sodium-aluminum hydroxide according to Eq. (2) [38]. The progress of the process was monitored through continuous measuring of the electric conductivity of the solution, which tends to decrease, once the solid is added and during stirring, until reaching a value close to 70% of the initial one and remaining stable. Then, the solution was filtered off the solids, and a new circle of mixing with fresh NaOH solution was initiated. The process was repeated 4 times, until electric conductivity value did not change with the addition of new NaOH solution. It has to be noted that the purpose of the process was to eliminate cyanides and free fluorides, and, through this, to render the sample safe for further treatment; destruction kinetics or side reactions that occur in this complex system was beyond the scope of this research. Analysis of the sample content in fluorides and cyanides ensured successful detoxification.

$$2NaCN + 5H_2O_2 \rightarrow 2NaOH + 2CO_2 \uparrow + N_2 \uparrow + 4H_2O \quad (1)$$

$$Na_3AlF_6 + 4NaOH \rightarrow 6NaF + NaAl(OH)_4 \quad (2)$$

Flotation

Flotation experiments were carried out in a Denver D1 laboratory flotation device, using 1.5 l cell. First, 150 g of dry sample and 750 ml of fresh water were added in the cell and pH was controlled by the addition of NaOH or H_2SO_4 solution. Subsequently, kerosene was added in the cell and conditioning was carried out at 500 rpm for 5 min. Methyl Isobutyl Carbinol (MIBC) frother was added and conditioning continued for 2 more minutes at 1000 rpm. In certain cases, Na_2SiO_3 solution was added as silica

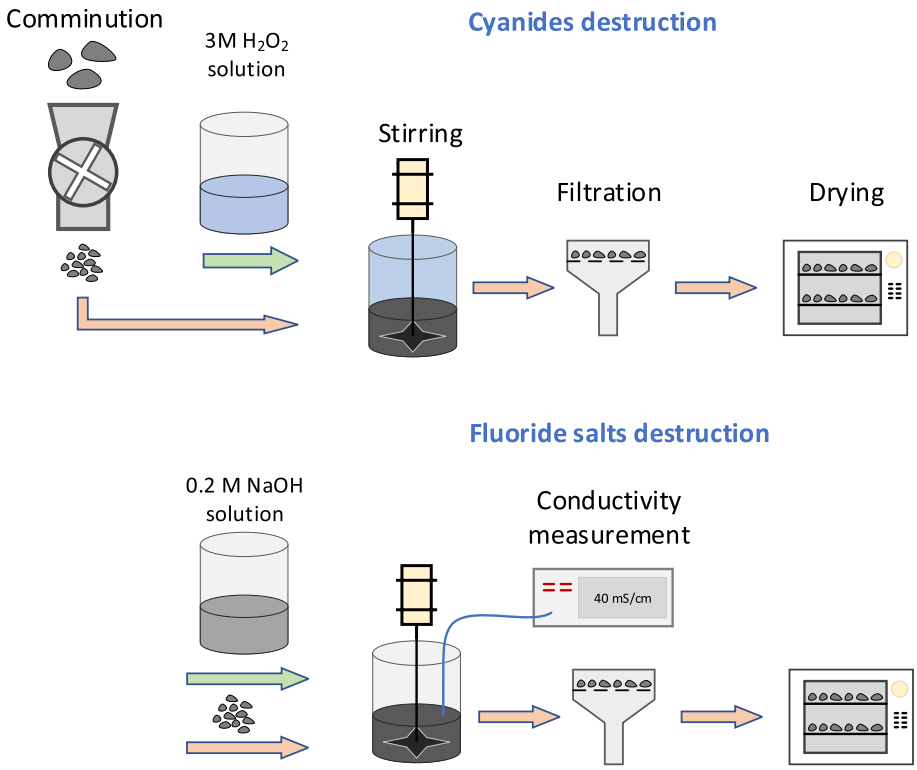

Fig. 2 Cyanide destruction and fluoride salts removal procedure through treatment with H_2O_2 and NaOH solution, respectively [19]

Table 2 List of modifiers used in the flotation process

Chemical	CAS number	Purpose
Kerosene, Sigma-Aldrich, USA	8008-20-6	Collector
Methyl Isobutyl Carbinol (MIBC), (≥ 98.5 wt%), Arkema, France	108-11-2	Frother
Na_2SiO_3 solution, Sigma-Aldrich, USA	1344-09-8	Siliceous minerals depressant
NaOH 0.5 M solution, Merck, USA	1310-73-2	pH regulators
H_2SO_4 solution (≥ 98 wt%), Merck, USA	7664-93-9	

Table 3 Experimental conditions and material properties

Parameter	Value
Kerosene dosage	250, 500, 750, and 1000 g/t
Na_2SiO_3 dosage	0, 200, 400, 600, and 800 g/t
MIBC dosage	200 g/t
pH	4, 6, 8, 10, 11
Sample mass	150 g
Conditioning time	5 min (collector) + 2 min (frother) + 2 min (Si depressant)
Flotation time	2.5–3.5 min
Pulp density	0.2 kg/l
Size of feed	− 90 µm, 90–420 µm
Impeller speed	1000 rpm

depressant at this stage prolonging the mixing procedure by 2 min. The pH was measured again and adjusted, if needed. All experiments were conducted at 25 ± 0.5 °C until demineralized froth was achieved. The flotation products were collected, dried, and weighted. A list of type and role of the chemical modifiers used in the flotation tests is presented in Table 2.

The performance of the flotation process was investigated in terms of four major process parameter, namely pH, collector dose, siliceous minerals depressant dose, and feed particle size (− 90 µm and 90–420 µm). D50 and D80 of the − 90 µm sample were 58 and 73 µm, respectively; similarly for the sample with particle size 90–420 µm, D50 and D80 were 247 and 325 µm, correspondingly. The conditions of the flotation experiments are presented in Table 3. In all cases, a dense and stable froth layer of about 4 cm thickness was created, as depicted in Fig. 3, ensuring smooth progress of the flotation process. The efficiency of the separation was evaluated through measuring carbon content and recovery in the concentrates. Additionally, since the main focus of the process is to remove aluminosilicates derived from the 2nd cut from graphite, the concentrate content in silicon and its distribution were also measured and presented.

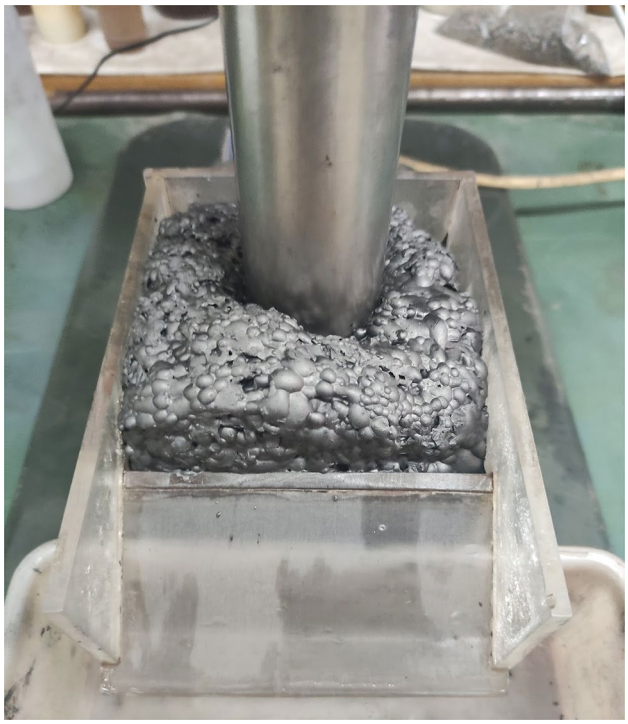

Fig. 3 Graphite froth flotation

Table 4 Chemical composition of SPL sample before and after detoxification procedure

Oxide	Content (wt%)	
	As received	After alkaline extraction
Na_2O	8.30	5.32
MgO	0.35	0.37
Al_2O_3	6.37	5.26
SiO_2	11.20	13.89
P_2O_5	0.06	0.07
K_2O	0.68	0.59
CaO	2.30	2.02
TiO_2	0.15	0.14
Fe_2O_3	0.87	0.71
F	3.25	1.86
Other	0.30	0.09
C_{tot}	66.16	69.98
LOI	67.92	70.29

Results and Discussion

Feed Characterization

The chemical composition of the 1st cut sample, before and after detoxification, is presented in Table 4. Furthermore, the X-ray diffraction diagram after detoxification and the results obtained by the implementation of the Rietveld method are presented in Fig. 4 and Table 5, respectively. The sample mainly consists of carbon that reaches 66 and 70 wt% before and after detoxification, correspondingly. No amorphous carbon or other carbon phase were identified, except to the 2H and 3R hexagonal graphite phases. The carbon content of the sample is very close to LOI content. Any small deviation is attributed to the decomposition of calcite to calcium oxide and the emission of carbon dioxide occurring at approx. 790 °C under room conditions [39]. The amount of silicon and aluminum exceeds 19 wt% in total (as oxides). In line with that, the mullite and quartz phases, where most of the silicon is distributed, constitute approx. 13 and 2%, respectively, according to the mineralogical analysis of the sample. A reduction in fluoride content of the sample was achieved after alkaline treatment with NaOH solution. The fluoride content that was 3.25 wt% initially reduced to 1.86 wt% after the implementation of detoxification procedure. The presence of fluoride denotes that the decomposition of cryolite and other fluoride salts was not complete. Significant reduction in cyanides content was achieved after the treatment of the sample with H_2O_2 solution; the concentration of the leachate in free and total cyanides reduced from 542 and 342 mg/kg for untreated SPL to 21 and 18 mg/kg for detoxified one, respectively.

Figure 5a, b presents the morphology of whole grains and polished section of SPL sample (particle size in the range 90–400 μm), respectively, as well as EDS spectra and weight fraction in major elements for 3 locations of interest where main phases were identified. Furthermore, Fig. 5c presents EDS mapping for aluminum (Al), sodium (Na), silicon (Si), carbon (C), and fluorine (F). The sample mainly consists of graphite and mullite grains. Caustic treatment of the SPL sample has caused corrosion at the surface of the mullite. It is also shown that graphite grains are impregnated with fluoride salts/cryolite. The material builds up layers of up to approx. 2–5 μm thickness inside the graphite grain, and such layers are not accessible by the NaOH solution; thus, the material did not dissolve, and part of cryolite remained intact. The finding is confirmed by elemental mapping; fluoride and sodium layering were identified in the carbon

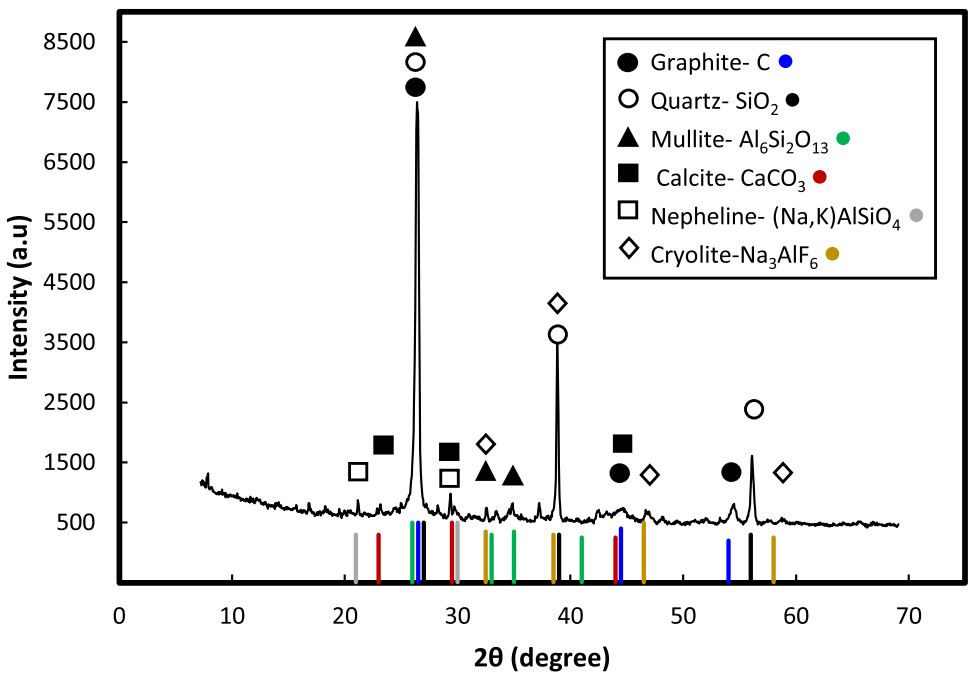

Fig. 4 X-ray powder diffraction diagram of SPL sample after detoxification and major standard XRD lines of identified phases

Table 5 Mineralogical composition of SPL sample after detoxification

Phase	Graphite C	Mullite $3Al_2O_3{\cdot}2SiO_2$	Calcite $CaCO_3$	Cryolite Na_3AlF_6	Nepheline (Na,K) $AlSiO_4$	Quartz SiO_2	Other
Content, wt%	69	13	5	5	3	2	3

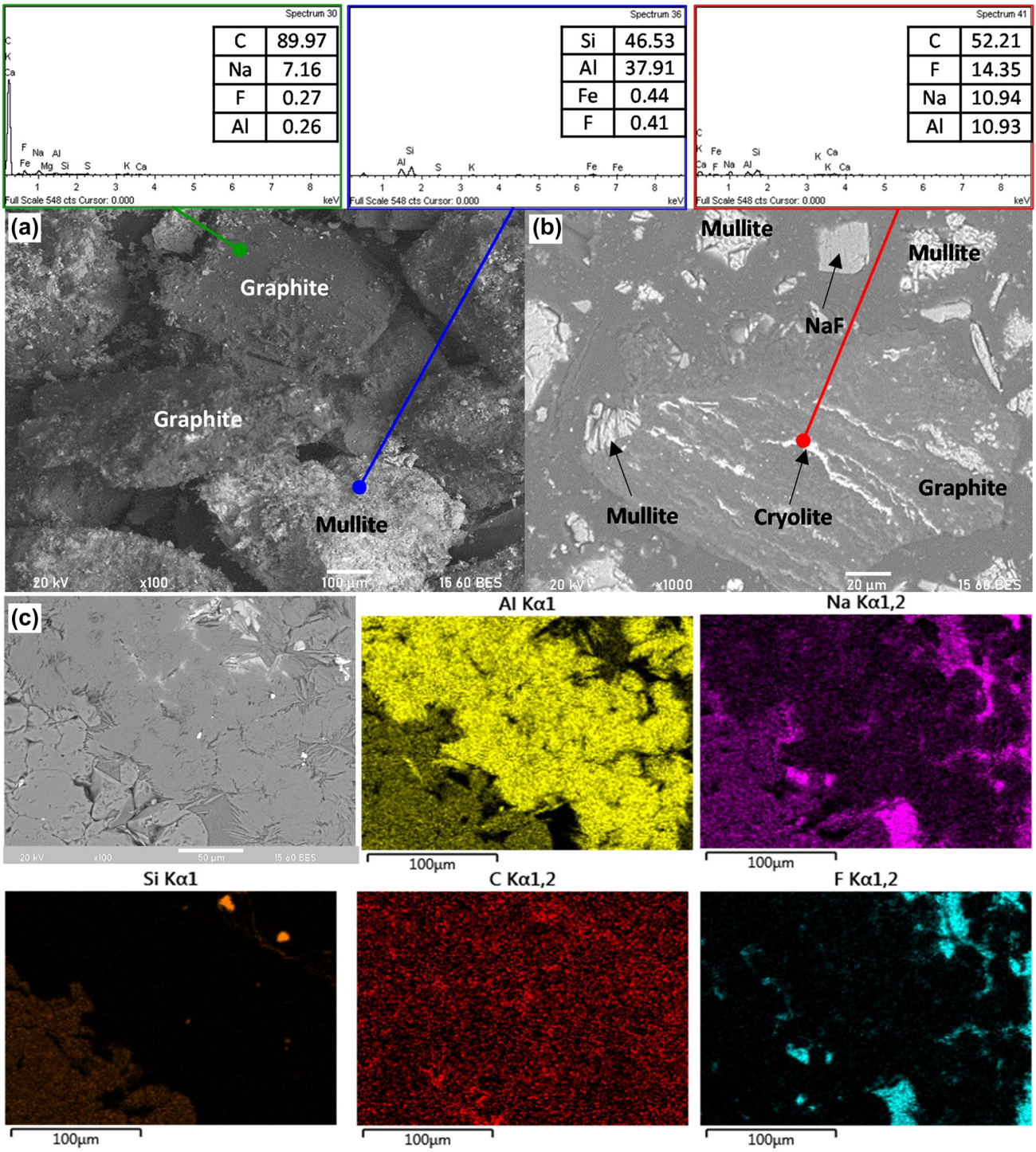

Fig. 5 SEM micrographs of **a** whole grain (X100), **b** thin section (X1000), and **c** EDS elemental mapping images (X100). EDS data provide mass fraction of each element

matrix. It is noteworthy that in most cases where F was identified also Na was present, thus denoting the existence of cryolite/sodium fluoride.

Figure 6 depicts carbon grade and recovery of float on heavy liquid with specific gravity 2.3 for SPL samples of various granulometry. It appears that both carbon content of the float and carbon recovery depend on granulometry of the feed. Among all samples of different sizes tested, the highest carbon recovery of 95.2% occurred for the finest one (− 210 µm) with carbon grade of 84.2 wt%; the sample

content in silicon is below 1 wt%, thus denoting that most of mullite ended up in the sinks. Maximum carbon content of 89.2 wt% was achieved in the sample with 210–420 µm granulometry, while carbon recovery appeared significantly reduced to 86.4% in comparison to the finest. The lowest carbon content of 77.6 wt% was determined in the coarse sample of 840–1190 µm particle size, with recovery reaching 90.4%. The silicon content on the float was determined to 4.2 wt%, denoting SiO_2 content of approx. 9 wt%. By compromising the values of grade and recovery of each float, the results show that efficient liberation is achieved for particle size − 420 µm.

Figure 7 presents XRD diagrams of all floats. Graphite and cryolite constitute the phases that were identified in all four samples. Mullite was identified in the floats of the samples with granulometry 420–840 µm and 840–1190 µm, as was expected due to their higher silicon content compared to that of the finer floats. Additionally, weak peaks that denote the presence of quartz were identified in the floats obtained for the sample 840–1190 µm. Supplementary Figure S-1 depicts the morphology of the sink and float for the 210–420 µm sample. In line with the results discussed before, it appears that the float consists mainly of graphite grains and also some white to gray unliberated phases of cryolite (Fig. S-1a). Sinks appear to have a radically different composition as revealed in Fig. S-1b. The sample mainly consists of mullite grains of characteristic yellow to brown color, along with some grains of white to gray color that could be cryolite, undissolved fluoride salts or even calcite. Moreover, the specific gravity of calcite and cryolite are 2.7 and 3.0, respectively; thus, it is normal that liberated grains of the aforementioned minerals sink along with mullite and quartz particles in heavy liquid with specific gravity of 2.3 [36]. Sinks also contain a considerable number of dark grains, some of which contain unliberated phases being distinguished because of color difference. Such phases are not always visible by naked eye because they are microscopically impregnated in the graphite phase. However, if gangue grade exceeds a certain level, the corresponding mixed grains sink.

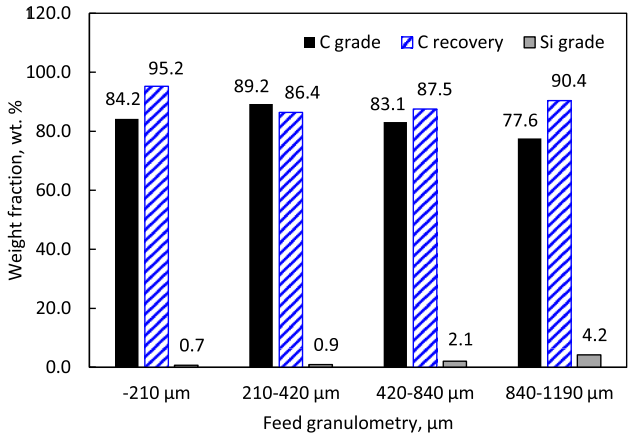

Fig. 6 Carbon and silicon grade and carbon recovery at the floating samples collected by the application of heavy liquid to SPL samples of different granulometry. The liquid specific gravity was 2.3

Froth Flotation

Effect of pH

The carbon grade and recovery of concentrates obtained from flotation, with pH value ranging between 4 and 11, are presented in Figs. 8a and b for feed particle size of − 90 µm and 90–420 µm, respectively, along with silicon grade (Fig. 8c) and recovery (Fig. 8d). The results denote that carbon grade and recovery are affected by

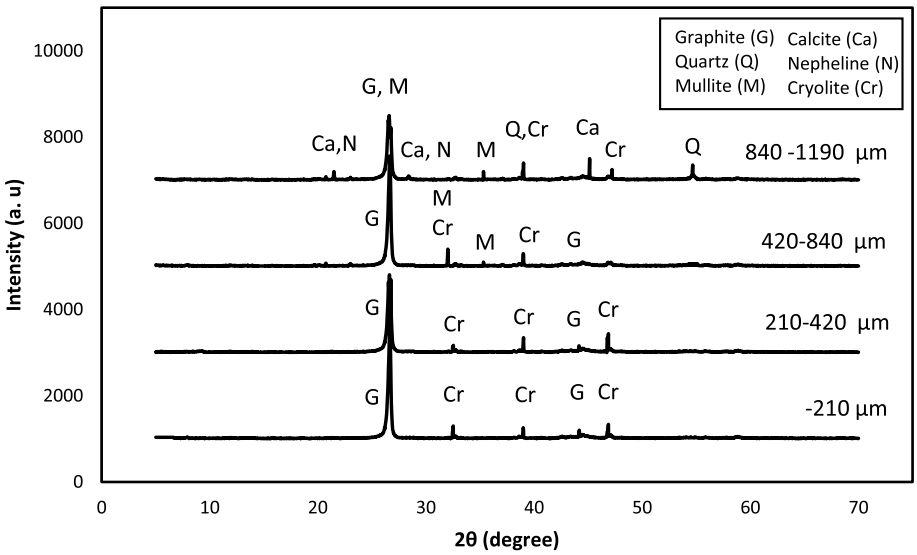

Fig. 7 X-ray powder diffraction diagrams of floats obtained through heavy liquid testing of SPL samples with different granulometry

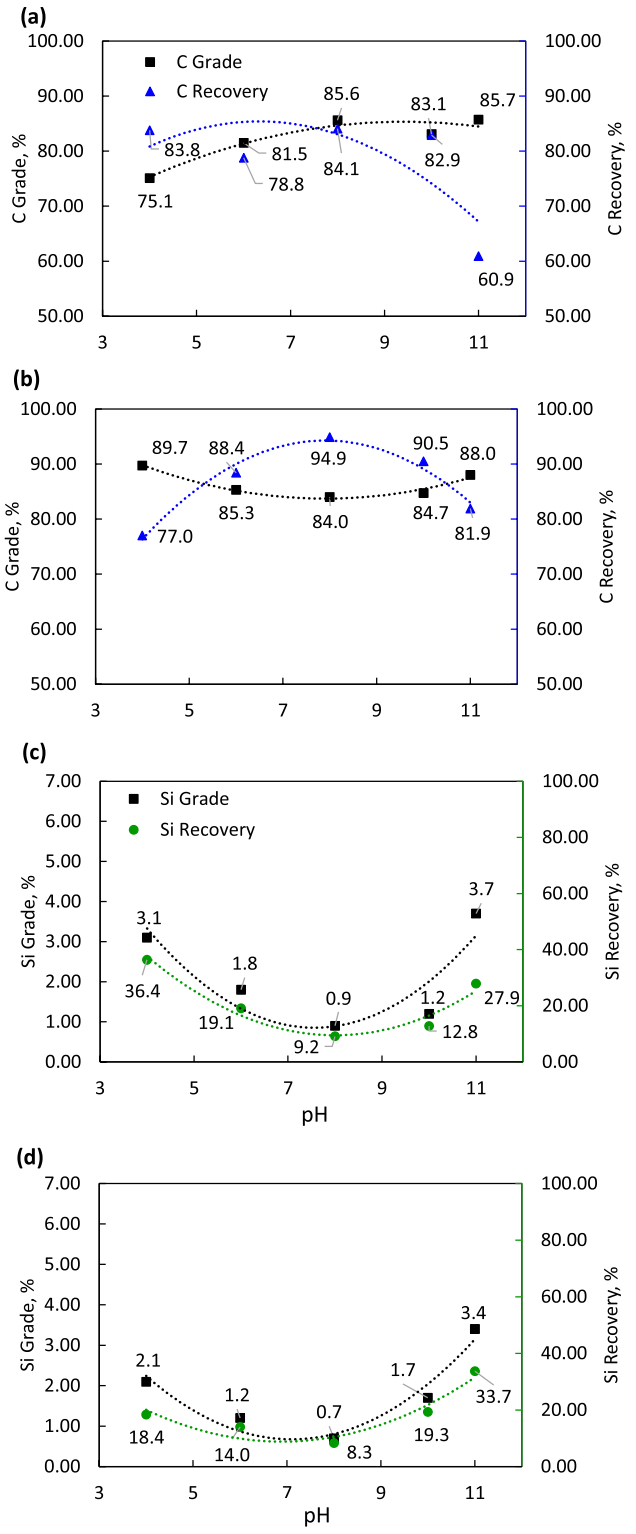

Fig. 8 Effect of pH on grade and recovery of carbon concentrate for − 90 µm (**a**) and 90–400 µm (**b**) SPL particle size, and on Si grade and recovery for − 90 µm (**c**) and 90–400 µm (**d**) grade [Other parameters: Kerosene: 500 g/t, MIBC: 200 g/t, 1000 rpm]

the pH value; carbon grade in the concentrate increases from 75 to 85.6 wt%, when pH increases from 4 to 8 for the − 90 µm sample; beyond pH 8 it remains constant (Fig. 8a). The highest carbon recovery (approx. 84%) was achieved when flotation was carried out at pH 8, and the minimum, of almost 61%, for pH value 11. Regarding Si content in the concentrate, minimum value appears at pH 8 attaining grade of 0.9 wt%, thus indicating SiO_2 content below 2 wt% (Fig. 8c).

The effect of pH on carbon recovery and grade in the concentrate for sample with particle size of 90–420 µm is similar to the corresponding of the − 90 µm size fraction. Throughout the entire pH range investigated, carbon recovery is above 77%, while in the pH region between 8 and 10 recovery values exceed 90%; maximum value (almost 95 wt%) is achieved at pH 8. The silicon content of the concentrate is below 2 wt% when pH ranged between 6 and 10, with minimum value of 0.7 wt% occurring at pH 8. Hence, the results show that optimum carbon grade and recovery occur at pH 8 for both − 90 µm and 90–420 µm samples. This is in line with other published studies that indicate optimum pH range for graphite flotation between 7 and 10 [25, 40, 41] or 7.5–8.5 [42].

Table 6 presents the chemical grade of the concentrates obtained at pH 8 using samples of different granulometry, along with the % difference of each oxide compared to the feed composition (presented in Table 4). It is obvious that the concentrate content in silicon and aluminum oxide, which are the elements that compose mullite, is significantly lower compared to that of the feed; regarding silicon oxide, the content is reduced by 86.3 and 89.1% for feed particle size − 90 µm and 90–420 µm, respectively; for aluminum oxide its content is reduced by 73% and 44.1%. Cryolite hosts most of sodium, and its separation is more complex because it is trapped in thin layers in graphite grains. The content of concentrate and feed in other elements presents only minor differences; thus, it appears that the purification of graphite phase from the aluminosilicates is feasible through flotation.

The X-ray diffraction diagrams of SPL flotation products (feed granulometry 90–420 µm) at pH 8 are depicted in Fig. 9. The pattern of the concentrate shows that, in addition to graphite, nepheline and cryolite are present, while quartz, mullite as well as graphite were identified in the tailing.

Supplementary Figure S-2 presents microscope images of the products obtained after flotation of 90–440 µm particle size at pH 8. Concentrate consists of graphite granules of irregular shape and opaque gray to black color (Fig. S-2a). Only a few light gray and brown grains or spots

Table 6 Chemical composition of concentrates obtained at pH 8, and comparison with that of the feed (Table 4) for different feed particle sizes

Oxide	Feed granulometry			
	− 90 µm		+90–420 µm	
	Conc. grade (wt%)	% difference compared to the feed (Table 4)	Conc. grade (wt %)	% difference compared to the feed (Table 4)
Na_2O	5.47	2.8	5.52	3.8
MgO	0.34	− 8.1	0.31	− 16.2
Al_2O_3	1.42	− 73.0	2.94	− 44.1
SiO_2	1.90	− 86.3	1.51	− 89.1
P_2O_5	0.07	0	0.09	28.6
K_2O	0.67	13.6	0.55	− 6.8
CaO	1.72	− 14.9	2.12	5.0
TiO_2	0.15	7.1	0.16	14.3
Fe_2O_3	0.75	5.6	0.79	11.3
F	1.54	− 17.2	1.60	− 14.0
Other	0.37	–	0.41	–
C_{tot}	85.60	22.3	84.00	20

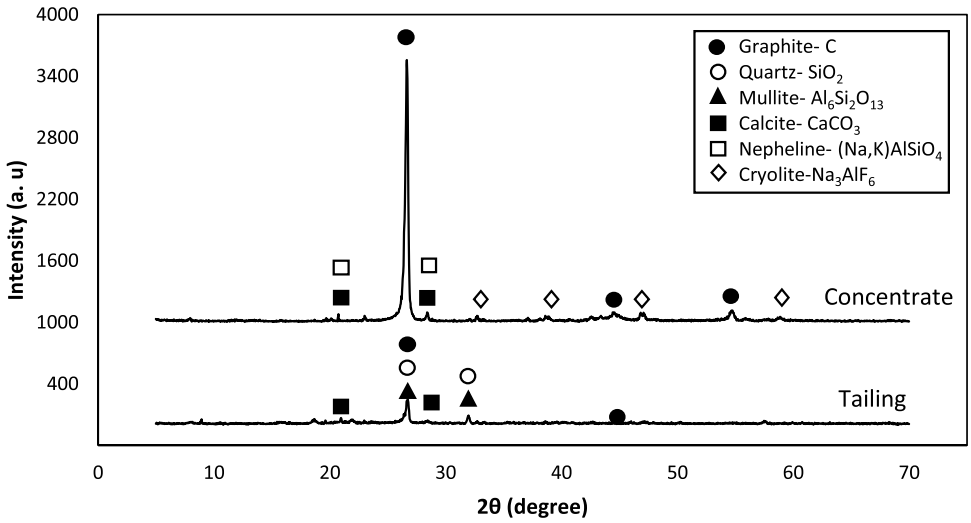

Fig. 9 X-ray powder diffraction diagrams of SPL flotation products at pH 8 for feed particle size 90–420 µm

on graphite grains are observed, which are either unliberated phases or gangue particles entrained in the froth. The appearance of tailing is radically different, mainly consisting of light to dark brown mullite grains, white to light gray grains (possibly calcite and liberated cryolite), and also some graphite grains that contain unliberated phases, which are recognizable due to their color difference (Fig. S-2b).

Effect of Kerosene Dosage

The effect of collector dose on carbon and silicon recovery in the concentrates obtained at pH of 8 is presented in the diagrams of Fig. 10 for both feed size fractions − 90 µm and 90–420 µm. Regarding the fine sample (− 90 µm), both carbon grade and recovery in the concentrate are maximized for kerosene dose of 500 g/t (Fig. 10a), with parallel silicon grade and recovery minimization, which attained values of 0.9 wt% and 9.2%, respectively (Fig. 10c). Higher kerosene dosage does not affect beneficially neither carbon recovery nor grade, while dose of 250 g/t is insufficient, since the silicon content reaches 6.1 wt%, denoting SiO_2 content in the concentrate of approx. 13 wt%, and carbon recovery only 28.0%. For the coarser sample, maximum recovery of almost 95% is achieved for kerosene dose of 500 g/t as well, while carbon grade reaches approx. 85 wt% (Fig. 10b). In that case, similarly to the fine sample, Si content in the concentrate reached 0.7 wt%, thus denoting SiO_2 content of 1.5 wt%. Higher kerosene dose causes marginal reduction of carbon recovery and increase of carbon grade; when kerosene dose is 250 g/t both grade and recovery deteriorated significantly. Regarding carbon content of the concentrate, it

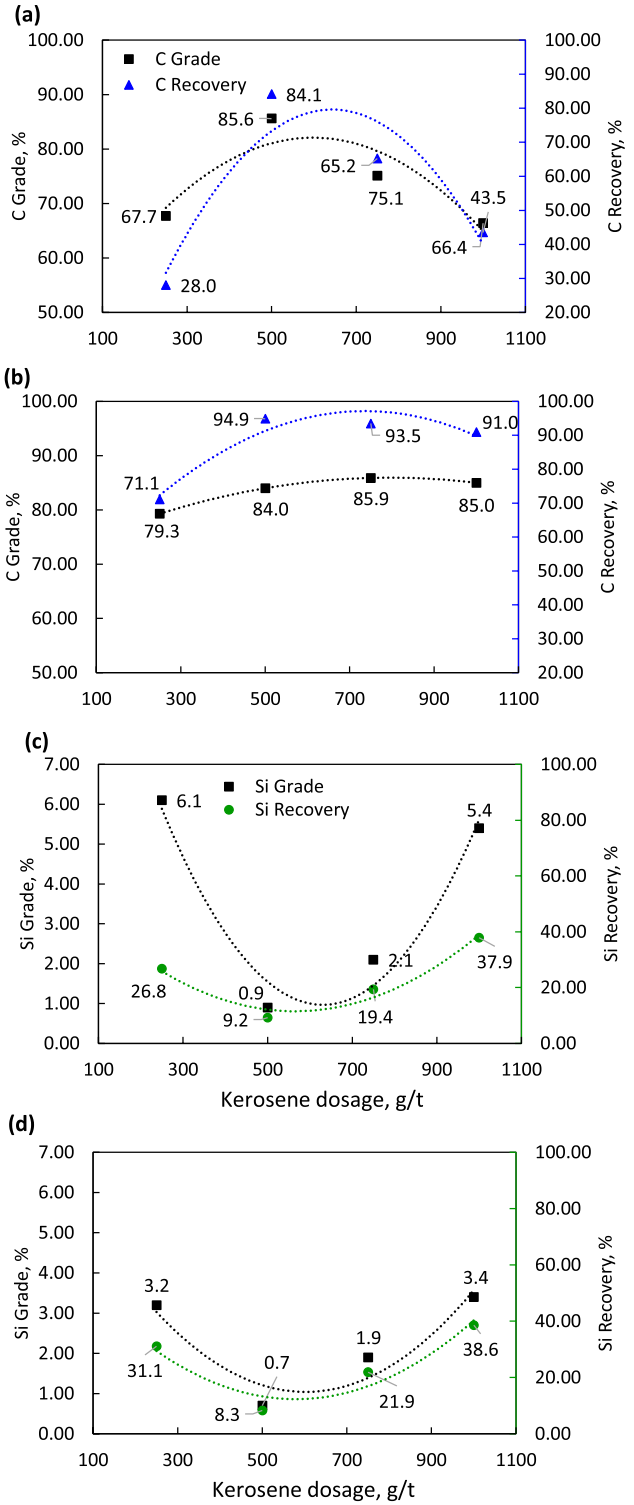

Fig. 10 Effect of kerosene dose on carbon grade and recovery of the concentrate for − 90 µm (**a**) and 90–400 µm (**b**) particle size, and on Si grade and recovery for − 90 µm (**c**) and 90–400 µm (**d**) [Other parameters: pH 8.00, MIBC: 200 g/t, 1000 rpm]

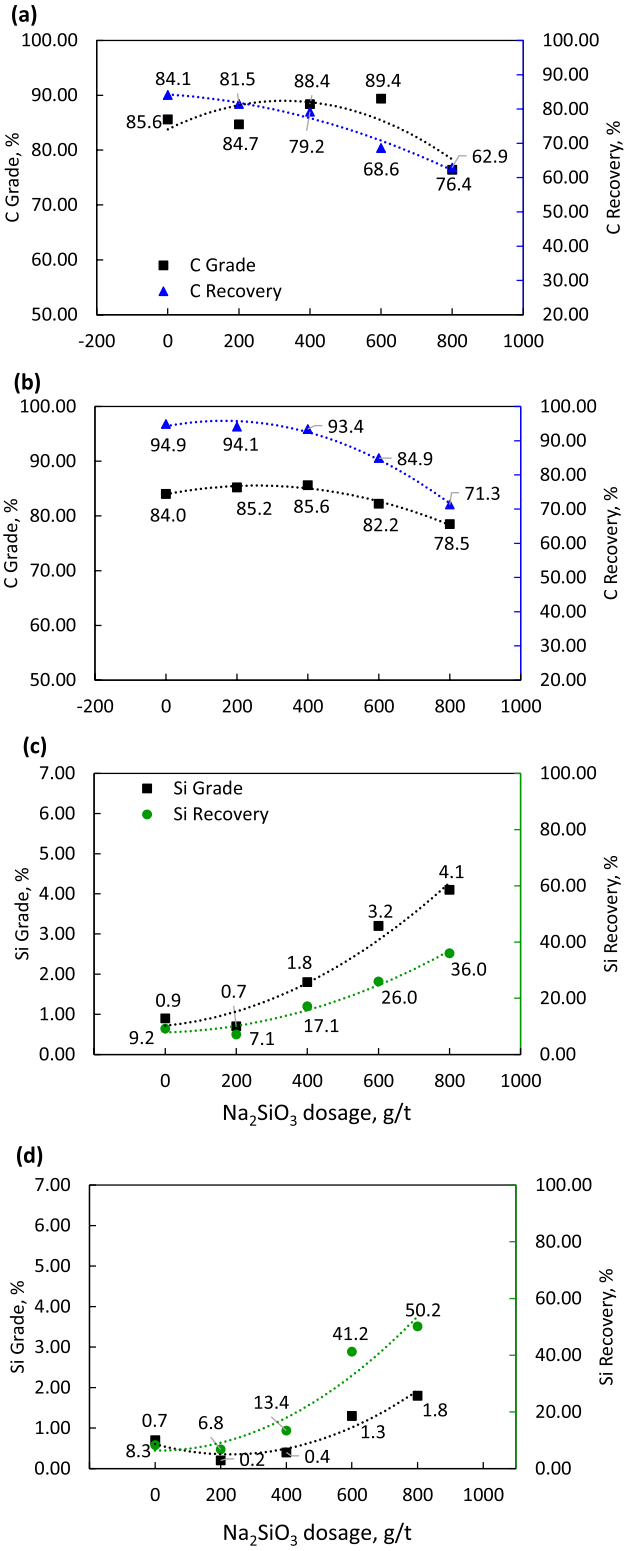

Fig. 11 Effect of Na_2SiO_3 dose on carbon grade and recovery of the concentrate for − 90 µm (**a**) and 90–400 µm (**b**) particle size, and on Si grade and recovery for − 90 µm (**c**) and 90–400 µm (**d**) particle size [Other parameters: kerosene: 500 g/t, pH 8.00, MIBC: 200 g/t, 1000 rpm]

reaches maximum value of about 86 wt% for kerosene dose of 750 g/t, with carbon recovery being 93.5%.

Effect of Na_2SiO_3 Addition

The effect of waterglass dose on carbon and silicon recovery and content in the concentrate for the fine sample (− 90 μm) is presented in Figs. 11a and c, and for the coarser (90–420 μm) in Figs. 11b and d. Regarding the fine sample, the carbon recovery is inversely proportional to the waterglass addition, with maximum recovery of 84.1% achieved when no waterglass is added while the minimum one (of almost 63%) for maximum waterglass dose (800 g/t). The concentrate with the highest carbon grade was achieved for waterglass dose of 400 g/t, reaching 88.4 wt% at the expense of the recovery, which was 79.2%. Compared to the case where no waterglass is added and the concentrate content in silicon is 0.9 wt%, the addition of waterglass in dose of 200 g/t causes marginal reduction in silicon content of the concentrate to 0.7 wt%. When waterglass dose is equal or higher than 600 g/t, a significant reduction in both carbon recovery and grade is observed, causing also increase in silicon content in the concentrate over 3.2 wt% (almost 6.9 wt% of SiO_2). Regarding the coarser sample, carbon content and recovery are practically the same in the concentrate that was obtained without waterglass, and those obtained through the addition of waterglass in dose of 200 and 400 g/t. Similar to the fine sample, the addition of waterglass to a dose of 600 g/t or more causes significant reduction in carbon grade and recovery, and a parallel increase in silicon recovery above 40% in the concentrate.

Conclusions

The study investigated the efficiency of flotation for the selective recovery of graphite from SPL containing considerable amount of mullite; the material originates from refractories and insulation lining of the Hall–Héroult cell. SPL was initially subjected to proper pretreatment process aiming to destroy cyanides and reduce free fluorides and thus render the material safe for experimentation.

The selective recovery of graphite through flotation was satisfactory. Best results were obtained at pH 8 and kerosene dose of 500 g/t, where carbon grade and recovery were 85.6 wt% and 85.1% for the fine sample (− 90 μm), and 84 wt% and 94.9% for the sample with particle size 90–420 μm, respectively. Samples of similar carbon grade and recovery were obtained through heavy liquid testing of same SPL grades, thus ensuring smooth flotation operation. Mullite and quartz were effectively separated in flotation since the concentrates content in silicon was below 1 wt% for both concentrates. The use of traditional Si depressant (waterglass) did not affect considerably the quality of the concentrate when added in small doses, while, dosage over 400 g/t deteriorated flotation results, causing considerable reduction of graphite recovery. Sodium fluorides and cryolite are the main impurities in the concentrates forming fine layers with thickness of a few microns. Further improvement of the obtained grade seems possible by combining grinding of graphite concentrates and subsequent NaOH treatment to create paths for reaching and finally dissolving the impurities.

Supplementary Information The online version contains supplementary material available at https://doi.org/10.1007/s40831-021-00453-0.

Acknowledgements The authors acknowledge Dr. Elias Chatzitheodoridis, Prof. in the field of Mineralogy-Petrology, for his valuable contribution in microscopic images, and Dr Mateja Košir, researcher at ZAG (Slovenian National Buildings and Civil Engineering Institute) for SEM-EDS mapping. The research was carried out under the project "SPL-Cycle Closing the loop of the Spent Pot-line (SPL) in the Al smelting process," a KIC Added Value Activity funded by the European Institute of Innovation and Technology (EIT) Raw Materials (PN 17141). EIT is a body of the European Union's Horizon 2020 Research and Innovation Program.

Declarations

Conflict of interest On behalf of all authors, the corresponding author states that there is no conflict of interest.

References

1. Courbariaux Y, Chaouki J, Guy C (2004) Update on spent potliners treatments: kinetics of cyanides destruction at high temperature. Ind Eng Chem Res 43(18):5828–5837
2. Lisbona DF, Steel KM (2008) Recovery of fluoride values from spent pot-lining: precipitation of an aluminium hydroxyfluoride hydrate product. Sep Purif Technol 61(2):182–192
3. Lossius LP, Øye HA (2000) Melt penetration and chemical reactions in 16 industrial aluminum carbon cathodes. Metall Mater Trans B 31(6):1213–1224
4. Holywell G, Breault R (2013) An overview of useful methods to treat, recover, or recycle spent potlining. JOM 65(11):1441–1451
5. Mikša D, Homšak M, Samec N (2003) Spent potlining utilisation possibilities. Waste Manag Res 21(5):467–473
6. Øye HA (2017) Discussion of industrial spent pot lining treatment. In: Proc 35th Int ICSOBA Conf., pp 2–5
7. Birry L, Poirier S (2020) The LCL&L process: a sustainable solution for the treatment and recycling of spent pot lining. Miner Met Mater Ser 1237–1242
8. Li W, Chen X (2010) Development status of processing technology for spent potlining in China. Light Met 1064–1066
9. Samec N, Mikša D, Kokalj F (2004) Recycling possibilities of spent potlining from the aluminum industry. Waste Manag Environ 78:347–356
10. Gomes V, Drumond P, Neto J, Lira A (2016) Co-processing at cement plant of spent potlining from the aluminum industry. Essent Readings Light Met 1057–1063

11. Grieshaber KW, Philipp CT, Bennett GF (1994) Process for recycling spent potliner and electric arc furnace dust into commercial products using oxygen enrichment. Waste Manag 14(3–4):267–276
12. Augood D, Keiser J (1989) The use of spent potlining as flux in making steel. Light Met Miner Met Mater Soc 395–398
13. Flores IV, Fraiz F, Lopes Junior RA, Bagatini MC (2019) Evaluation of spent pot lining (SPL) as an alternative carbonaceous material in ironmaking processes. J Mater Res Technol 8(1):33–40
14. von Krüger P (2011) Use of Spent Potlining (SPL) in ferro silico manganese smelting. Light Met 2011:275–280
15. Wang Y, Chen X, Zhang S, Yang P (2020) Recycling of spent pot lining first cut from aluminum smelters by utilizing the two-step decomposition characteristics of dolomite. Materials 13(22):1–9
16. Yu D, Paktunc D (2019) Carbothermic reduction of chromite fluxed with aluminum spent potlining. Trans Nonferr Met Soc China 29(1):200–212
17. Moxnes B, Gikling H, Kvande H, Rolseth S, Straumsheim K (2003) Addition of refractories from spent potlining to alumina reduction cells to produce Al-Si alloys. In: Light metals 2003, The Minerals, Metals & Materials Society, pp 329–334
18. Personnet P (1999) Treatment and reuse of spent pot lining, an industrial application in a cement kiln. In: Light metals 1999, The Minerals, Metals & Materials Society, pp 1049–1056
19. Angelopoulos PM, Klinar D, Kosir M, Ebin B, Bremerstein I, Peys A et al (2020) A novel, zero-waste technology for spent pot lining recycling. In: Proceedings of the 38th International ICSOBA Conference, pp 739–749
20. Wakamatsu T, Numata Y (1991) Flotation of graphite. Miner Eng 4(7–11):975–982
21. Raghavan P, Chandrasekhar S, Sivam C, Lalithambika M, Damodaran AD (1992) Removal of ultrafine graphite impurities from china clay by floc-flotation. Int J Miner Process 36(1–2):51–61
22. Gredelj S, Zanin M, Grano SR (2009) Selective flotation of carbon in the Pb-Zn carbonaceous sulphide ores of Century Mine. Zinifex Miner Eng 22(3):279–288
23. Vasumathi N, Vijaya Kumar TV, Ratchambigai S, Subba Rao S, Bhaskar RG (2015) Flotation studies on low grade graphite ore from eastern India. Int J Min Sci Technol 25(3):415–420
24. Peng W, Qiu Y, Zhang L, Guan J, Song S (2017) Increasing the fine flaky graphite recovery in flotation via a combined multiple-treatments technique of middlings. Minerals 7(11):208
25. Chehreh Chelgani S, Rudolph M, Kratzsch R, Sandmann D, Gutzmer J (2016) A review of graphite beneficiation techniques. Miner Process Extr Metall Rev 37(1):58–68
26. Bulatovic S (2015) Handbook of flotation reagents: Chemistry, theory and practice. Flotation of Industrial Minerals. Elsevier, Amsterdam
27. Gaudin AM (1957) Flotation, 2nd edn. McGraw-Hill, New York
28. Lewis RH (1970) Graphite. In: Mineral facts and problems, Bulletin No 650. US Bureau of Mines
29. Schönfelder I, Gock E, Tochtrop E, Rieder S (2015) Recycling von Elektrolyseausbruch (SPL) aus der Primäraluminiumgewinnung. Recycl und Rohstoffe 8:385–404
30. Tropenauer B, Klinar D, Samec N, Golob J, Kortnik J (2019) Sustainable waste-treatment procedure for the spent potlining (SPL) from aluminium production. Mater Technol 53(2):277–284
31. Li H, Feng Q, Ou L, Long S, Cui M, Weng X (2013) Study on washability of microcrystal graphite using float-sink tests. Int J Min Sci Technol 23(6):855–861
32. Lechler P, Desilets M (1987) A review of the use of loss on ignition as a measurement of total volatiles in whole-rock analysis. Chem Geol 63:341–344
33. ASTM D7348–13 (2013) Standard Test Methods for Loss on Ignition (LOI) of Solid Combustion Residues. West Conshohocken
34. ISO 14403–2 (2018) Water quality—determination of total cyanide and free cyanide using flow analysis (FIA and CFA)—Part 2: Method using continuous flow analysis
35. Doebelin N, Kleeberg R (2015) Profex: a graphical user interface for the Rietveld refinement program BGMN. J Appl Crystallogr 48:1573–1580
36. Mindat.org webpage. https://www.mindat.org/. Accessed 27 April 2021
37. Kitis M, Akcil A, Karakaya E, Yigit NO (2005) Destruction of cyanide by hydrogen peroxide in tailings slurries from low bearing sulphidic gold ores. Miner Eng 18(3):353–362
38. Tropenauer B, Klinar D, Golob J (2021) Improved understanding of Sodium hydroxide concentration role and kinetic model of cryolite reactive extraction in cathode Spent Pot Linings. Pol J Chem Technol 23(1):37–44
39. Karunadasa KSP, Manoratne CH, Pitawala HMTGA, Rajapakse RMG (2019) Thermal decomposition of calcium carbonate (calcite polymorph) as examined by in-situ high-temperature X-ray powder diffraction. J Phys Chem Solids 134:21–28
40. Ravichandran V, Eswaraiah C, Manisankar P (2012) Beneficiation of low grade graphite ore deposits of Tamilnadu (India). Ultra Chem 8(2):159–168
41. Jara AD, Betemariam A, Woldetinsae G, Kim JY (2019) Purification, application and current market trend of natural graphite: a review. Int J Min Sci Technol 29(5):671–689
42. Crozier RD (1992) Flotation: theory, reagents and ore testing. Pergamon, Oxford